ORIGINAL ARTICLE

Early Cardiac Involvement Affects Left Ventricular Longitudinal Function in Females Carrying α-Galactosidase A Mutation

Role of Hybrid Positron Emission Tomography and Magnetic Resonance Imaging and Speckle-Tracking Echocardiography

BACKGROUND: Hybrid ^{18}F-fluorodeoxyglucose (FDG) positron emission tomography and magnetic resonance imaging may differentiate mature fibrosis or scar from fibrosis associated to active inflammation in patients with Anderson-Fabry disease, even in nonhypertrophic stage. This study was designed to compare the results of positron emission tomography and magnetic resonance cardiac imaging with those of speckle-tracking echocardiography in heterozygous Anderson-Fabry disease females.

METHODS AND RESULTS: Twenty-four heterozygous females carrying α-galactosidase A mutation and without left ventricular hypertrophy underwent cardiac positron emission tomography and magnetic resonance using ^{18}F-FDG for glucose uptake and 2-dimensional strain echocardiography. ^{18}F-FDG myocardial uptake was quantified by measuring the coefficient of variation (COV) of the standardized uptake value using a 17-segment model. Focal ^{18}F-FDG uptake with COV >0.17 was detected in 13 patients, including 2 patients with late gadolinium enhancement at magnetic resonance. COV was 0.30±0.14 in patients with focal ^{18}F-FDG uptake and 0.12±0.03 in those without (P<0.001). Strain echocardiography revealed worse global longitudinal systolic strain in patients with COV >0.17 compared with those with COV ≤0.17 (−18.5±2.7% versus −22.2±1.8%; P=0.024). For predicting COV >0.17, a global longitudinal strain >−19.8% had 77% sensitivity and 91% specificity and a value >2 dysfunctional segments 92% sensitivity and 100% specificity.

CONCLUSIONS: In females carrying α-galactosidase A mutation, focal ^{18}F-FDG uptake represents an early sign of disease-related myocardial damage and is associated with impaired left ventricular longitudinal function. These findings support the hypothesis that inflammation plays an important role in glycosphingolipids storage disorders.

Letizia Spinelli, MD
Massimo Imbriaco, MD
Carmela Nappi, MD
Emanuele Nicolai, MD
Giuseppe Giugliano, MD
Andrea Ponsiglione, MD
Tommaso Claudio
    Diomiaiuti, BSC
Eleonora Riccio, MD, PhD
Giovanni Duro, MD
Antonio Pisani, MD, PhD
Bruno Trimarco, MD
Alberto Cuocolo, MD

CLINICAL PERSPECTIVE

Anderson-Fabry disease is a rare, X-linked, lysosomal storage disorder characterized by mutations in the gene encoding enzyme α-galactosidase A synthesis, which results in cell storage of globotriaosylceramide. In females carrying α-galactosidase A mutation, disease phenotype can be detected only by the presence of disease signs or by the demonstration of globotriaosylceramide storage within target organs. Cardiac involvement, which is the major contributor to mortality, is characterized by ventricular hypertrophy, dysfunction, and focal myocardial fibrosis. We studied 24 heterozygous female patients with Anderson-Fabry disease without left ventricular hypertrophy who underwent hybrid cardiac positron emission tomography and magnetic resonance using ^{18}F-fluorodeoxyglucose and 2-dimensional strain echocardiography. Abnormal fluorodeoxyglucose uptake was noted in 13 patients corresponding to impaired left ventricular longitudinal systolic strain. These data suggest that inflammation as it relates to pathogenesis of cardiac dysfunction may be the pathological link between cardiomyocyte globotriaosylceramide storage and development of disease-related cardiomyopathy. An extensive use of 2-dimensional strain echocardiography may be advocated for the initial evaluation of patients with α-galactosidase A mutation to identify early cardiac involvement.

Anderson-Fabry disease (AFD) is a rare, lysosomal storage disorder characterized by mutations in the gene encoding the enzyme α-Gal A (α -galactosidase A), which results in a deficiency in enzyme activity,[1] leading to cell storage of globotriaosylceramide. Females carrying a-Gal A mutation usually manifest clinical disease and have a reduction in life expectancy of ≈10 years.[2–7] Skewed inactivated X chromosome or cross-induction are considered as mechanisms potentially underlying the clinical expression of heterozygous females.[8–10] Given that plasma or leukocytes α-Gal A activity may be within normal range, disease phenotype can be detected only by the presence of disease signs or by the demonstration of glycosphingolipids storage within target organs. Early preclinical disease identification is highly important as it might indicate preventive enzyme replacement therapy before the onset of irreversible organ damage.[11,12] Plasma lyso-globotriaosylceramide, a useful prognostic marker of disease severity and progression in affected males, is difficult to correlate with disease burden in female patients with isolated manifestation of organ involvement.[13,14] Cardiac imaging techniques can detect AFD-related cardiac damage, potentially in an early stage. Cardiac magnetic resonance (MR) imaging is an attractive tool for diagnosing cardiac involvement in AFD, because of its ability to detect early subtle tissue changes and to assess cardiac fibrosis by using late gadolinium enhancement (LGE) technique.[15–17] Short time inversion recovery (STIR) imaging enables detection of myocardial edema with high diagnostic accuracy.[18] On the other hand, ^{18}F-fluorodeoxyglucose (FDG) positron emission tomography (PET) is a noninvasive molecular imaging technique that is highly sensitive to metabolically active processes that use glucose as a source of energy.[19,20] Using hybrid PET-MR cardiac imaging in a small sample of AFD patients, we previously observed a focal myocardial ^{18}F-FDG uptake, suggesting inflammation, even in nonhypertrophic stage.[21] Studies using speckle-tracking echocardiography agree in demonstrating that left ventricular (LV) systolic function is impaired in AFD patients, despite a preserved ejection fraction and even at early phase of disease.[22–25] This study was designed to compare the results of hybrid PET-MR cardiac imaging with those of speckle-tracking echocardiography in heterozygous AFD females.

METHODS

The data, analytic methods, and study materials will not be made available to other researchers for purposes of reproducing the results or replicating the procedure.

Study Population

Between January 2014 and February 2017, we enrolled 24 females (mean age, 37±12 years) with genetically proven AFD from 11 unrelated families, who did not present cardiac symptoms. No patient had received enzyme replacement therapy before study entry. Exclusion criteria were pregnancy, breast-feeding, and standard contraindication for MR imaging. As part of the baseline examination, the clinical team collected information from each patient on traditional cardiovascular risk factors (including age, body mass index, hypercholesterolemia, diabetes mellitus, hypertension, or smoking) and on history of AFD-associated pain in hands and feet, decreased sweating, gastrointestinal problems and neurological symptoms (including stroke and headache). Coronary artery disease was ruled out based on the clinical history plus a negative maximal exercise electrocardiography stress test or pharmacological stress echocardiography. In each patient, renal function was investigated by measuring glomerular filtration rate and 24-hour urine protein excretion. Each patient underwent hybrid PET-MR study and speckle-tracking echocardiography within a week. A cohort of 24 age-matched healthy women undergoing only echocardiography served as control group. This group consisted of healthy volunteers or outpatient subjects referred for non-specific symptoms and in whom a detailed diagnostic workup and clinical follow-up was unremarkable. Another cohort of 10 age-matched control women who underwent PET imaging for other reasons served as control group to determine normal

^{18}F-FDG uptake. They had no evidence of active inflammatory, coronary or valvular diseases, of diabetes mellitus or severe hepatic, renal, malignant and hematologic diseases and were not receiving corticosteroids. All patients provided informed and written consent. The study conformed to the principles outlined in the Declaration of Helsinki and was approved by the local Ethics Advisory Committee.

Biomarker Measurements

Blood samples were obtained in all patients for determination of cardiac troponin by high-sensitivity cardiac troponin I assay (Abbott ARCHITECT STAT) and of NT-proBNP (N-terminal pro-B-type natriuretic peptide) by a sandwich immunoassay on an Elecsys 2010 (Roche Diagnostics, Basel, Switzerland). After centrifugation (30 minutes, 3000 relative centrifugal force, 4°C), samples were frozen at −80°C until assayed in a blinded fashion. The normal upper limit values were 15.6 pg/mL for high-sensitivity cardiac troponin I and 253 pg/mL for NT-proBNP.

PET-MR Imaging

All patients underwent cardiac PET-MR hybrid imaging (Biograph mMR; Siemens Healthcare, Erlangen, Germany) according to the Society of Nuclear Medicine and Molecular Imaging and the American Society of Nuclear Cardiology guidelines for cardiac PET computed tomography.[26] To ensure optimal suppression of ^{18}F-FDG uptake, patients were instructed to consume 2 high-fat, low carbohydrate meals the day before the study and then fasted for at least 6 hours before the test.[27] All patients were intravenously injected with 370 MBq of ^{18}F-FDG, and imaging was performed 45 minutes later. Standard cardiac MR imaging protocol sequences were performed for morphological and functional studies, including T2-weighted STIR sequences, phase-sensitive inversion recovery, and true fast imaging with steady-state precession. Early and late enhancement inversion recovery sequences were obtained from 5 to 15 minutes after administration of a 0.15-mmol/kg body weight gadolinium-diethylenetriaminepentaacetic acid (Magnevist; Schering, Berlin, Germany) bolus.[28,29] An inversion time scout scan was acquired, and the optimal inversion time value was found. Cine, T2, and gadolinium-enhanced acquisitions were ECG triggered and performed in breath-hold. Patients were scanned in the supine position. A single bed position PET emission scan was acquired over 20 minutes simultaneously with a whole heart MR sequence.

PET-MR Analysis

A radiologist and a nuclear medicine physician in consensus analyzed cardiac PET-MR images on a dedicated workstation, as previously described.[21] Morphological and functional MR data were analyzed to assess LV anatomy, kinetic, wall thickness, and early and LGE patterns. PET images were classified according to ^{18}F-FDG uptake pattern: homogeneous, heterogeneous, and focal. Images with a homogeneous or a heterogeneous pattern show the outline of the LV wall with uniform or inconsistent tracer distribution, respectively, whereas images with a focal pattern show a segmental increase in tracer uptake. Only focally increased cardiac uptake was considered a positive finding for the presence of active cardiac inflammation.[21] The standardized uptake value (SUV) was

also determined. The intensity of ^{18}F-FDG uptake was quantified by measuring the SUV in 17 myocardial segments, and the average SUV and SD of the SUV were calculated for each patient. The coefficient of variation (COV) of the SUV in each patient was calculated as the SUV SD divided by the average SUV as an index of heterogeneity of ^{18}F-FDG uptake.[20] Two nuclear medicine physicians blindly measured SUV, and the measurements were averaged. The intraobserver and interobserver variability of SUV measurements were <5%. In control subjects, mean COV and SD values were 0.12 and 0.025, respectively. Therefore, a COV value >0.17 was considered as an index of abnormal tracer uptake. LGE and T2-weighted STIR images were compared with PET images using source data and fused images according to 17-segment model of LV.

Echocardiography

Echocardiography was performed using commercially available ultrasound equipment (M4S probe, Vivid 7; GE Vingmed Ultrasound AS, Horten, Norway). Tissue Doppler was used to record mitral annular early diastolic peak velocities at the septal and lateral walls, with the measurements being averaged. Apical 2-, 3-, and 4-chamber views were obtained with the highest possible frame rates to evaluate LV longitudinal strain, whereas parasternal short-axis views at basal and apical level were used to assess radial and circumferential strains.

Echocardiography Analysis

Standard echocardiography analysis was performed according to American Society of Echocardiography,[30] as previously described.[31] LV mass was calculated by Devereux formula and divided by body surface area to calculate LV mass index. A cutoff value ≤95 g/m^2 was used to determine normal LV mass index. Using 2- and 4-chamber views, LV end-systolic and end-diastolic volumes were measured by modified Simpson's method and ejection fraction was subsequently calculated, whereas left atrial volume was measured by biplane area–length formula and indexed to body surface area. Evaluation of diastolic function included tissue Doppler measurements.

Speckle-tracking echocardiography analysis was performed offline by using dedicated software (Echo Pac version BT12.0.0, GE Vingmed Ultrasound) by averaging the measurements obtained from 3 consecutive cardiac cycles. By analyzing LV according to a 17-segment model, both segmental and global systolic longitudinal strains were calculated. Peak global systolic radial and circumferential strain profiles were measured in both short-axis planes. The speckle-tracking echocardiography reproducibility of our laboratory has been previously published.[31]

Statistical Analysis

Results are expressed as mean±SD or medians and interquartile range or proportions. The Kolmogorov–Smirnov test was used to evaluate if the continuous variables fit a normal distribution. Age-matched control subjects were selected by frequency matching. For comparison of groups, unpaired t test or Wilcoxon rank-sum test were performed depending on whether the distribution was normal or not. Receiver operating characteristic analysis was used to determine the best cutoff value of global longitudinal strain and sum of dysfunctional segments (ie, longitudinal strain >−15%) to

identify a COV >0.17. A *P* value <0.05 was considered statistically significant.

RESULTS

The individual demographic and genetic data of AFD patients are reported in Table 1. The mutation c.901C>G was present in 4 patients from 2 different families. As far it was possible to extend the pedigree analysis, no link between families sharing the same mutation was found. According to selection criteria, all patients carrying α-Gal A mutation had normal LV mass index, some reported mild neuropathic pain and isolated episodes of gastrointestinal complaints and 2 patients had cornea verticillata with normal visual acuity. No patient was affected by diabetes mellitus.

PET-MR Imaging

MR procedure was successfully performed in all individuals without any side effects. No patients showed early gadolinium enhancement. Only 2 patients had LGE, one of them with T2–STIR positive at precontrast phase. The remaining 22 patients exhibited no evidence of LGE and T2–STIR negative. ^{18}F-FDG PET imaging revealed no uptake in 2 patients, homogeneous uptake in 9, and focal uptake localized in the lateral region in 13, including the 2 patients with LGE. No patients showed heterogeneous tracer uptake. The COV was 0.30±0.14 in patients with focal ^{18}F-FDG uptake and 0.12.8±0.03 in those without ($P<0.001$). Figure 1 shows an example of myocardial LGE in the lateral LV wall at cardiac MR and focal uptake on the corresponding ^{18}F-FDG PET images.

Echocardiographic Findings in Control Subjects and Heterozygous AFD Patients

The anthropometric characteristics and echocardiographic findings of control subjects and heterozygous AFD patients, considered as a whole and categorized according to PET results, are summarized in Table 2. There was no statistically significant difference in body

Table 1. Genetic Characteristics of 24 Females With Anderson-Fabry Disease

| Patient	Family	Age (y)	α-GAL A Mutation	α-GAL A Protein Effect	Reference
1	1	21	IVS4+5G>T	Splicing alteration	…
2	1	47	IVS4+5G>T	Splicing alteration	…
3	2	66	c.667T>G	p.C223E	…
4	3	33	c.680G>C	p.R227P	Zizzo et al,[32] 2016
5	4	22	c.1066C>T	p.R356W	Ishii et al,[33] 2007
6	5	32	c.1021dupG	Frameshift and premature stop codon	…
7	6	34	c.424T>C	p.C142R	Topaloglu et al,[34] 1999
8	7	47	c.1066C>T	p.R356W	Ishii et al, 2007[33]
9	7	53	c.1066C>T	p.R356W	Ishii et al,[33] 2007
10	7	38	c.1066C>T	p.R356W	Ishii et al,[33] 2007
11	8	48	c.901C>G	p.R301G	Shabbeer et al,[35] 2002
12	8	19	c.901C>G	p.R301G	Shabbeer et al,[35] 2002
13	8	33	c.901C>G	p.R301G	Shabbeer et al,[35] 2002
14	9	43	c.352C>T	p.R118C	Spada et al,[36] 2006
15	9	50	c.352C>T	p.R118C	Spada et al,[36] 2006
16	9	48	c.352C>T	p.R118C	Spada et al,[36] 2006
17	9	51	c.352C>T	p.R118C	Spada et al,[36] 2006
18	10	30	c.1021dupG	Frameshift and premature stop codon	…
19	10	44	c.1021dupG	Frameshift and premature stop codon	…
20	10	49	c.1021dupG	Frameshift and premature stop codon	…
21	11	29	c.680G>C	p.R227P	Zizzo et al,[32] 2016
22	12	27	c.863C>A	p.A288D	Eng et al,[37] 1994
23	13	30	c.508G>A	p.D170N	…
24	14	23	c.901C>G	p.R301G	Shabbeer et al,[35] 2002

α-Gal A indicates α-galactosidase A.
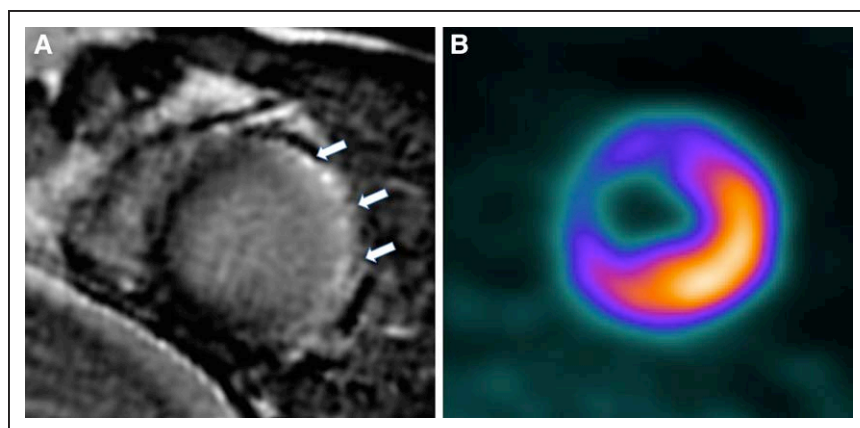
Figure 1. Cardiac magnetic resonance and 18F-fluorode-oxyglucose positron emission tomography (PET) images in a representative study patient.
A, Late gadolinium enhancement (LGE) in the lateral left ventricular wall (white arrows). **B**, Corresponding PET showing focal tracer uptake matching the area of LGE.

mass index, heart rate, blood pressure, and renal function between the 2 groups. A mild proteinuria was detected in heterozygous AFD patients, with values >150 mg/24 hours in 8 patients (33.3%), whereas no urine protein excretion was found in control group (*P*<0.001). Values of high-sensitivity cardiac troponin I and NT-proBNP were within normal range in heterozygous AFD patients. The standard echocardiographic measurements, namely LV mass index, geometry pattern, ejection fraction, and Doppler-derived diastolic parameters and the results from 2-dimensional strain echocardiography were comparable in heterozygous AFD patients and control subjects.

LV Longitudinal Function and 18F-FDG PET Findings

When AFD population was categorized according to 18F-FDG PET results, patients with COV >0.17 did not differ from patients with COV ≤0.17 on age, body mass index, renal function, levels of urine protein, or NT-proB-NP. The values of high-sensitivity cardiac troponin I tended to be higher in patients with COV ≤0.17, without reaching a statistical significance (Table 2). The 2 groups

showed similar values of heart rate, blood pressure, and measurement from standard echocardiography (Table 3). No relation between segmental longitudinal strain and segmental SUV values was found (*P*=0.39), but global longitudinal systolic strain was significantly worse in patients with COV >0.17 when compared with those with COV ≤0.17. Conversely, both radial and circumferential strains did not differ between groups. Each patient with COV >0.17 exhibited at least 1 segment with longitudinal strain >−15% (range 1–11), whereas no patient with COV ≤0.17 did. A significant difference between patients with COV ≤0.17 and those with COV >0.17 was observed in the values of longitudinal strain from the basal-inferoseptal (*P*=0.004) and midinferoseptal (*P*=0.014) segments. Figure 2 shows 18F-FDG PET-MR images and LV myocardial longitudinal strain bull's-eye rendering from 3 representative AFD patients. For predicting COV >0.17, a global longitudinal strain >−19.8% had 77% (95% confidence intervals, 43%–95%) sensitivity and 91% (95% confidence interval, 62%–100%) specificity and a value >2 dysfunctional segments 92% (95% confidence interval, 62%–100%) sensitivity and 100% (95% confidence interval, 74%–100%) specificity.

Table 2. Clinical Data From Control Subjects and AFD Patients According to 18F-Fluorodeoxyglucose Positron Emission Tomography Results

	Control Subjects (n=24)	AFD Patients (n=24)	*P* Value	AFD With COV≤17 (n=11)	AFD With COV>17 (n=13)	*P* Value
Age, y	35±10	37.2±12.2	0.53	37.5±14	36.8±11	0.86
Body mass index, kg/m²	22±2.8	24±3.6	0.67	27±3.4	23±3.9	0.12
GFR, mL min⁻¹ 1.73 m⁻²	120±10	106±18	0.17	105±21.9	107±14.2	0.90
Urine protein, mg/24 h	…	123 (100–180)	…	126 (0.20–250)	120 (100–180)	0.82
HS-troponin I, pg/mL	…	1.32±4.29	…	0.015±0.02	2.42±5.69	0.17
NT-proBNP, pg/mL	…	64.2±37.2	…	63.8±37.4	64.6±36.9	0.95
Heart rate, bpm	71.3±8.5	72.1±12.9	0.56	69.5±10.2	74.3±15	0.37
Systolic blood pressure, mm Hg	119.3±11.2	117.1±18.9	0.77	121.8±13	113.1±21	0.25
Diastolic blood pressure, mm Hg	73.2±9.3	72.3±12.6	0.76	76.8±11.5	69.5±12.1	0.19

Values are presented as mean±SD or median (interquartile range). AFD indicates Anderson-Fabry Disease; COV, coefficient of variation; GFR, glomerular filtration rate; HS, high sensitivity; and NT-proBNP, N-terminal pro-B-type natriuretic peptide.

Table 3. Echocardiographic Parameters From Control Subjects and AFD Patients According to ^{18}F-Fluorodeoxyglucose Positron Emission Tomography Results

	Control Subjects (n=24)	AFD Patients (n=24)	P Value	AFD With COV≤17 (n=11)	AFD With COV>17 (n=13)	P Value
LV mass index, g/m²	80.7±5.7	80.9±14.7	0.81	82.7±14.3	79.1±15.5	0.77
Relative wall thickness	0.36±0.04	0.37±0.04	0.78	0.36.6±0.03	0.37.3±0.05	0.83
LV end-diastolic volume, mL	86±11	85±19	0.80	89±22	80.5±16	0.77
LV end-systolic volume, mL	29±7	30±7	0.72	31±8	29±6	0.76
LV ejection fraction, %	63±5	65±2.6	0.76	65±2	64±3	0.92
Left atrial volume, mL/m²	28±3.5	29±3.7	0.77	28.4±4.3	30.4±3.6	0.06
Mitral E/A	1.6±0.3	1.2±0.4	0.12	1.1±0.3	1.4±0.5	0.42
E/Ea	6.8±2.4	7.1±2.2	0.42	6.9±2.8	7.6±1.8	0.62
Systolic pulmonary pressure, mm Hg	23.2±3	25.5±2.8	0.62	25±3.1	26±2.5	0.85
Global longitudinal strain, %	−21±2.3	−20.4±2.8	0.11	−22±1.8	−18.5±2.7	0.01
Basal circumferential strain, %	−20±2	−19.3±5.7	0.62	−20.4±5.2	−18.9±6.2	0.46
Apical circumferential strain, %	−21±3	−19.5±5.5	0.21	−19.8±6.1	−18.9±4.9	0.77
Basal radial strain, %	35±9	29.3±7.6	0.13	28.8±8.2	29.8±7.1	0.82
Apical radial strain, %	29±5	27.2±6.8	0.53	29±6.1	25.2±7.5	0.37

Values are presented as mean±SD. AFD indicates Anderson-Fabry Disease; COV, coefficient of variation; E/A, ratio between early and late filling; E/Ea, ratio between mitral inflow E wave and mitral annulus early diastolic velocity; and LV, left ventricular.

DISCUSSION

Cardiac ^{18}F-FDG PET imaging revealed focal myocardial uptake in a large percentage of female patients carrying α-Gal A mutation and with normal LV mass. Cardiac MR imaging did not detect any abnormalities in most of patients with focal myocardial ^{18}F-FDG uptake. Longitudinal strain by 2-dimensional strain echocardiography was significantly impaired in patients who displayed a focal myocardial ^{18}F-FDG uptake. AFD is associated with storage of glycosphingolipids in endothelial cells and in cells of several organs, including the skin, kidneys, peripheral nervous system, and heart.[1] Cardiac involvement is the major contributor to mortality in AFD, and it is characterized by LV hypertrophy and dysfunction as the result of intramyocyte accumulation of glycosphingolipids (disease-related myocardial damage). Heterozygous women often do not demonstrate low enzyme activity and show later organ and tissue involvement when compared with male patients. Sometimes, women can be an exclusive carrier of mutation, without a disease phenotype. Given the building evidence showing that early administration of enzyme replacement therapy has the best chance of protecting against the effects of AFD on myocardial function and LV mass, early detection of cardiac involvement is important.[11,12] Endomyocardial biopsy can demonstrate accumulation of globotriaosylceramide in the myocardium of patients without LV hypertrophy, offering proof of myocardial involvement.[38] However, endomyocardial biopsy would be difficult to do serially because of higher cost, invasiveness, and potential sampling errors. Taking in mind that noninvasive diagnosis of myocardial

damage in AFD is a challenging issue, we investigated a cohort of female patients lacking LV hypertrophy with hybrid PET-MR imaging and speckle-tracking echocardiography. We found LGE in a small subset of patients, in keeping with previous observation that female AFD patients have susceptibility of developing late enhancement in the early stages, before hypertrophy.[39] In AFD-related cardiomyopathy, LGE is thought to represent focal fibrosis, according to histological correlation.[40] The demonstration of severe and irreversible fibrosis in myocardium of patients carrying the mutation, IVS4+919G>A, before development of LV hypertrophy or other significant cardiac manifestations, contributed to strengthen the relatively recent concept of fibrosis before hypertrophy.[41] The imaging approach combining LGE and T2-weighted STIR has proved to detect edema, an important hallmark of reversible myocardial inflammatory injury, in several clinical conditions.[42–45] Diagnosis of myocardial inflammation is based on the presence of at least 2 of the following MR findings: (1) myocardial edema detected by T2-weighted STIR; (2) myocardial hyperemia detected by early gadolinium enhancement technique; and (3) myocardial damage with nonischemic pattern detected by LGE.[46] A high variation in sensitivity and negative predictive value has been reported, reflecting the intrinsic drawbacks of current diagnostic criteria, which are mainly based on the use of conventional cardiac MR sequences.[47] In our study, only in 1 patient, positive T2-weighted STIR sequences on the myocardium surrounding an area of focal LGE was observed. Nevertheless, focal myocardial ^{18}F-FDG uptake was present not only in patients with T2–STIR positive or with LGE but also in up to 50%

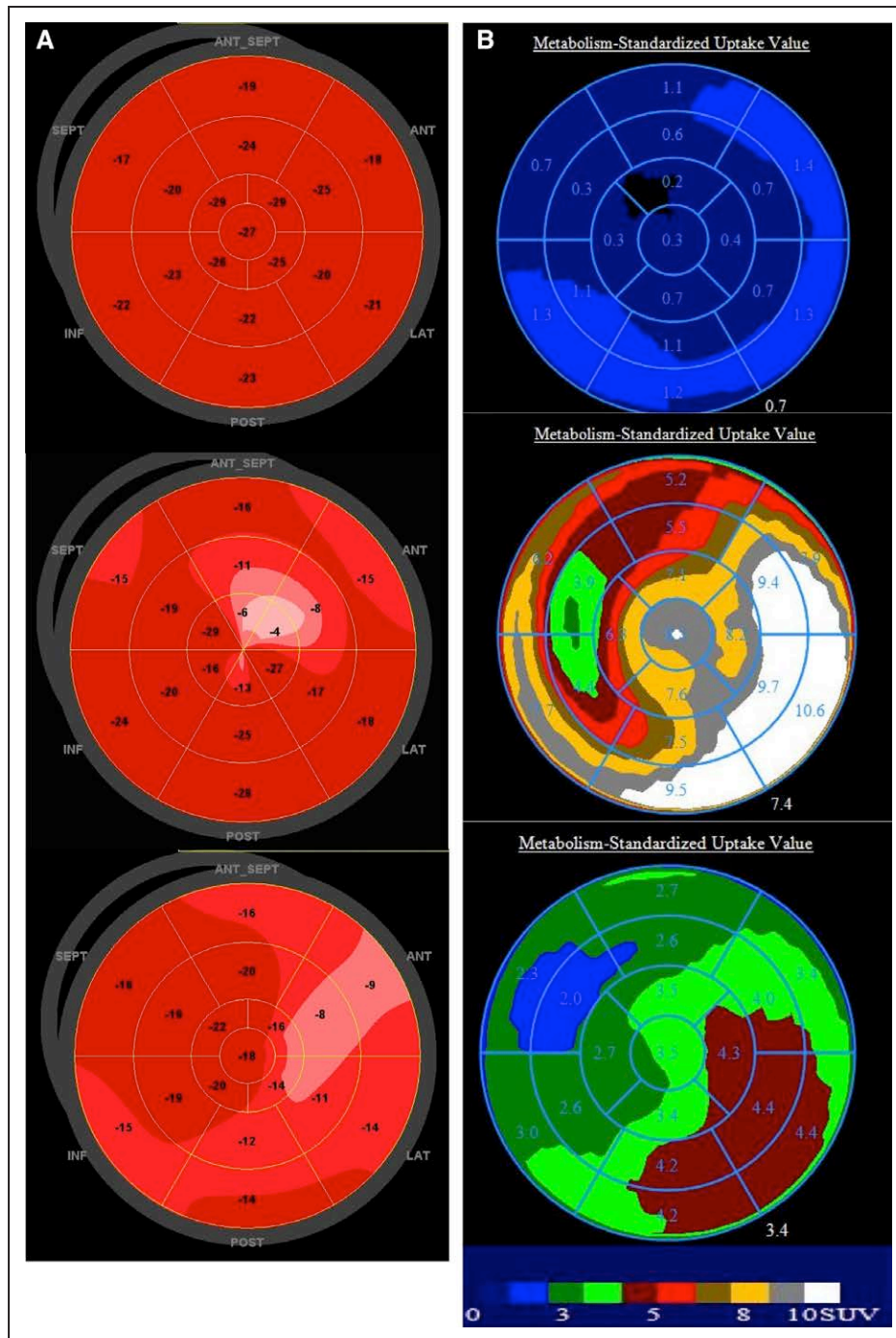**Figure 2. Speckle-tracking echocardiography and 18F-fluorodeoxyglucose (FDG) positron emission tomography in three representative study patients.**
A, Bull's-eye rendering of left ventricular longitudinal strain and (**B**) polar map of [18]F- FDG standardized uptake value (SUV). **Upper**, Patient with homogeneous ^{18}F-FDG uptake and negative magnetic resonance (MR) imaging. Global longitudinal strain (GLS) was −23.1% and coefficient of variation (COV) 0.11. **Middle**, Patient with focal ^{18}F-FDG uptake and negative MR imaging. GLS was −17.5% and COV 0.38. **Lower**, Patient with focal ^{18}F-FDG uptake and late gadolinium enhancement on MR imaging. GLS was −15.3% and COV 0.29. SEPT indicates septal; LAT, lateral; ANT, anterior; INF, inferior; and POST, posterior.

of patients who did not display MR abnormalities. The negative results of T2-weighted STIR imaging in most of patients showing ^{18}F-FDG uptake abnormalities are not surprising as the abnormalities in PET and MR imag-

ing rely on different mechanisms. Cardiac ^{18}F-FDG PET has proven to be an accurate diagnostic tool with an incremental value in identifying active inflammation as it provides metabolic information, a valuable comple-

ment to the information on heart anatomy and myocardial structure provided by MR imaging.[28,48,49]

Sensitivity of cardiac MR in patients with myocardial inflammation is heterogeneous.[50] It correlates with the extent of cardiomyocyte necrosis promoting an expansion of interstitial space,[48] when compared with PET that is based on the ^{18}F-FDG uptake by hypermetabolic glucose-avid tissue. Taken together, our findings confirm and expand the hypothesis that phlogosis may play a crucial role for AFD-related myocardial damage.[21,51] In vitro and in vivo studies demonstrated that cell accumulation of globotriaosylceramide induces oxidative stress (including lipid peroxidation) and inflammation.[52–54] Inflammatory macrophages infiltration has been documented in endomyocardial biopsy specimens from AFD patients.[55] Inflammation is present in all tissues and may be associated with other potentially pathological processes such as apoptosis, impaired autophagy, which could all contribute synergistically to tissue damage.[56] Nordin et al[51] assessed T2 mapping and troponin in a cohort of AFD patients, most of them with LV hypertrophy, and concluded that inflammation related to cardiomyocyte globotriaosylceramide storage contributed to LGE. In our study, the finding that the presence of myocardial focal ^{18}F-FDG uptake was not associated to increased levels of troponin suggests that troponin is not a marker of very early cardiac involvement in AFD patients. Interestingly, global longitudinal strain was able to detect subclinical LV dysfunction associated to PET abnormalities. Echocardiography is largely used for the assessment of cardiac involvement in AFD, given its ease of access. The measurement of longitudinal systolic strain can be obtained in an easy, valuable, and reproducible way by using speckle-tracking echocardiography, a technique that offers several advantages over tissue Doppler imaging because its measurements are angle independent and, thus, suitable for a regional assessment of deformation of all myocardial segments.[57] Longitudinal strain is impaired earlier than circumferential and radial strains, in the case of myocardial damage.[22] Previous studies demonstrated reduced global longitudinal strain in AFD patients lacking LV hypertrophy.[23–25] Our study corroborates these observations and highlights the link between impairment of LV longitudinal function and myocardial metabolic abnormalities in early phase of AFD-related cardiomyopathy. Thus, in women carrying α-Gal A mutation, the suspicion of early-stage cardiac involvement should arise in the presence of impaired global longitudinal strain or even of reduced longitudinal strain in several myocardial segments, inducing to a deeper investigation. However, it is worth underscoring that the cutoff values obtained for longitudinal strain should be considered pertinent only to a female population. Further studies are warranted to demonstrate the reliability of LV longitudinal function parameters for detection of early cardiac involvement in children or young male AFD patients. Furthermore,

caution should be used when applying our results to the imaging obtained with the use of other ultrasound equipments, despite the low variability between different machine and software vendors.[58]

Limitations and Strengths

The relatively small sample size could represent a limitation for the present results, but it reflects the rarity of the clinical condition under evaluation and the single-center nature of the study. On the other hand, evidence that the baseline characteristics of patients included in the present study were quite similar to those of patients included in studies by other authors[23–25] makes our findings wide generalizable. The use of imaging techniques able to assess cardiac metabolism, structure, and function represents a major strength of the study. Yet, criteria applied for analysis of both ^{18}F-FDG PET and cardiac MR are well established and validated in clinical studies. Another possible limitation of the present study is that up to 20% of patients have inadequate suppression despite various dietary preparations and longer fasting periods could be helpful to avoid nonspecific myocardial uptake.[27] Finally, T1 and T2 mapping assessment could be helpful. Recent studies showed that decreased native myocardial T1 is highly prevalent in AFD patients even prior the onset of LV hypertrophy.[59,60]

Conclusions

The present study demonstrates the relation between impaired LV longitudinal function and myocardial metabolic abnormalities detected by hybrid PET-MR imaging in early phase of AFD-related cardiomyopathy. These findings advocate an extensive use of 2-dimensional strain echocardiography as initial evaluation of patients with α-Gal A mutation. Cardiac ^{18}F-FDG PET could gain use in detecting myocardial inflammation that likely represents a clue of response to cardiomyocyte globotriaosylceramide storage. It is possible to hypothesize that a focal ^{18}F-FDG uptake in young patients carrying AFD-related mutation may be a predictor of the development of LV hypertrophy, although further research is needed to establish this issue.

Correspondence

Letizia Spinelli, MD, Department of Advanced Biomedical Sciences, University of Naples Federico II, Via Pansini 5, 80131 Naples, Italy. E-mail letspine@unina.it

Affiliations

Departments of Advanced Biomedical Sciences (L.S., M.I., C.N., G.G., A. Ponsiglione, B.T., A.C.) and Public Health (E.R., A. Pisani), University of Naples Federico II, Italy; SDN IRCCS, Naples, Italy (E.N., T.C.D.); and Institute of Biomedicine and Molecular Immunology, National Council of Research, Palermo, Italy (G.D.).

Disclosures

None.

REFERENCES

1. Zarate YA, Hopkin RJ. Fabry's disease. *Lancet*. 2008;372:1427–1435. doi: 10.1016/S0140-6736(08)61589-5.

2. Deegan PB, Baehner AF, Barba Romero MA, Hughes DA, Kampmann C, Beck M; European FOS Investigators. Natural history of Fabry disease in females in the Fabry Outcome Survey. *J Med Genet*. 2006;43:347–352. doi: 10.1136/jmg.2005.036327.

3. Wang RY, Lelis A, Mirocha J, Wilcox WR. Heterozygous Fabry women are not just carriers, but have a significant burden of disease and impaired quality of life. *Genet Med*. 2007;9:34–45. doi: 10.1097GIM.0b013e3180 2d8321.

4. Kampmann C, Baehner F, Whybra C, Martin C, Wiethoff CM, Ries M, Gal A, Beck M. Cardiac manifestations of Anderson-Fabry disease in heterozygous females. *J Am Coll Cardiol*. 2002;40:1668–1674.

5. Wilcox WR, Oliveira JP, Hopkin RJ, Ortiz A, Banikazemi M, Feldt-Rasmussen U, Sims K, Waldek S, Pastores GM, Lee P, Eng CM, Marodi L, Stanford KE, Breunig F, Wanner C, Warnock DG, Lemay RM, Germain DP; Fabry Registry. Females with Fabry disease frequently have major organ involvement: lessons from the Fabry Registry. *Mol Genet Metab*. 2008;93:112–128. doi: 10.1016/j.ymgme.2007.09.013.

6. Bouwman MG, Rombach SM, Schenk E, Sweeb A, Wijburg FA, Hollak CE, Linthorst GE. Prevalence of symptoms in female Fabry disease patients: a case-control survey. *J Inherit Metab Dis*. 2012;35:891–898. doi: 10.1007/s10545-011-9447-9.

7. MacDermot KD, Holmes A, Miners AH. Anderson-Fabry disease: clinical manifestations and impact of disease in a cohort of 60 obligate carrier females. *J Med Genet*. 2001;38:769–775.

8. Dobrovolny R, Dvorakova L, Ledvinova J, Magage S, Bultas J, Lubanda JC, Elleder M, Karetova D, Pavlikova M, Hrebicek M. Relationship between X-inactivation and clinical involvement in Fabry heterozygotes. Eleven novel mutations in the alpha-galactosidase a gene in the Czech and Slovak population. *J Mol Med (Berl)*. 2005;83:647–654. doi: 10.1007/s00109-005-0656-2.

9. Echevarria L, Benistan K, Toussaint A, Dubourg O, Hagege AA, Eladari D, Jabbour F, Beldjord C, De Mazancourt P, Germain DP. X-chromosome inactivation in female patients with Fabry disease. *Clin Genet*. 2016;89:44–54. doi: 10.1111/cge.12613.

10. Dobyns WB, Filauro A, Tomson BN, Chan AS, Ho AW, Ting NT, Oosterwijk JC, Ober C. Inheritance of most X-linked traits is not dominant or recessive, just X-linked. *Am J Med Genet A*. 2004;129A:136–143. doi: 10.1002/ajmg.a.30123.

11. Whybra C, Miebach E, Mengel E, Gal A, Baron K, Beck M, Kampmann C. A 4-year study of the efficacy and tolerability of enzyme replacement therapy with agalsidase alfa in 36 women with Fabry disease. *Genet Med*. 2009;11:441–449. doi: 10.1097/GIM.0b013e3181a23bec.

12. Weidemann F, Niemann M, Sommer C, Beer M, Breunig F, Wanner C. Interdisciplinary approach towards female patients with Fabry disease. *Eur J Clin Invest*. 2012;42:455–462. doi: 10.1111/j.1365-2362.2011.02614.x.

13. Smid BE, van der Tol L, Biegstraaten M, Linthorst GE, Hollak CE, Poorthuis BJ. Plasma globotriaosylsphingosine in relation to phenotypes of Fabry disease. *J Med Genet*. 2015;52:262–268. doi: 10.1136/jmedgenet-2014-102872.

14. Lenders M, Hennermann JB, Kurschat C, Rolfs A, Canaan-Kühl S, Sommer C, Üçeyler N, Kampmann C, Karabul N, Giese AK, Duning T, Stypmann J, Krämer J, Weidemann F, Brand SM, Wanner C, Brand E. Multicenter Female Fabry Study (MFFS) - clinical survey on current treatment of females with Fabry disease. *Orphanet J Rare Dis*. 2016;11:88. doi: 10.1186/s13023-016-0473-4.

15. Schulz-Menger J, Bluemke DA, Bremerich J, Flamm SD, Fogel MA, Friedrich MG, Kim RJ, von Knobelsdorff-Brenkenhoff F, Kramer CM, Pennell DJ, Plein S, Nagel E. Standardized image interpretation and post processing in cardiovascular magnetic resonance: society for cardiovascular magnetic resonance (SCMR) board of trustees task force on standardized post processing. *J Cardiovasc Magn Reson*. 2013;15:35. doi: 10.1186/1532-429X-15-35.

16. Moon JC, Sachdev B, Elkington AG, McKenna WJ, Mehta A, Pennell DJ, Leed PJ, Elliott PM. Gadolinium enhanced cardiovascular magnetic resonance in Anderson-Fabry disease. Evidence for a disease specific abnormality of the myocardial interstitium. *Eur Heart J*. 2003;24:2151–2155.

17. Kozor R, Grieve SM, Tchan MC, Callaghan F, Hamilton-Craig C, Denaro C, Moon JC, Figtree GA. Cardiac involvement in genotype-positive Fabry disease patients assessed by cardiovascular MR. *Heart*. 2016;102:298–302. doi: 10.1136/heartjnl-2015-308494.

18. h-Ici D, Ridgway JP, Kuehne T, Berger F, Plein S, Sivananthan M, Messroghli DR. Cardiovascular magnetic resonance of myocardial edema using a short inversion time inversion recovery (STIR) black-blood technique: diagnostic accuracy of visual and semi-quantitative assessment. *J Cardiovasc Magn Reson*. 2012; 14:22.

19. James OG, Christensen JD, Wong TZ, Borges-Neto S, Koweek LM. Utility of FDG PET/CT in inflammatory cardiovascular disease. *Radiographics*. 2011;31:1271–1286. doi: 10.1148/rg.315105222.

20. Rischpler C, Nekolla SG, Dregely I, Schwaiger M. Hybrid PET/MR imaging of the heart: potential, initial experiences, and future prospects. *J Nucl Med*. 2013;54:402–415. doi: 10.2967/jnumed.112.105353.

21. Nappi C, Altiero M, Imbriaco M, Nicolai E, Giudice CA, Aiello M, Diomiaiuti CT, Pisani A, Spinelli L, Cuocolo A. First experience of simultaneous PET/MRI for the early detection of cardiac involvement in patients with Anderson-Fabry disease. *Eur J Nucl Med Mol Imaging*. 2015;42:1025–1031. doi: 10.1007/s00259-015-3036-3.

22. Shanks M, Thompson RB, Paterson ID, Putko B, Khan A, Chan A, Becher H, Oudit GY. Systolic and diastolic function assessment in Fabry disease patients using speckle-tracking imaging and comparison with conventional echocardiographic measurements. *J Am Soc Echocardiogr*. 2013;26:1407–1414. doi: 10.1016/j.echo.2013.09.005.

23. Gruner C, Verocai F, Carasso S, Vannan MA, Jamorski M, Clarke JT, Care M, Iwanochko RM, Rakowski H. Systolic myocardial mechanics in patients with Anderson-Fabry disease with and without left ventricular hypertrophy and in comparison to nonobstructive hypertrophic cardiomyopathy. *Echocardiography*. 2012;29:810–817. doi: 10.1111/j.1540-8175.2012.01704.x.

24. Saccheri MC, Cianciulli TF, Lax JA, Gagliardi JA, Cáceres GL, Quarin AE, Kisinovsky I, Rozenfeld PA, Reisin RC; AADELFA. Two-dimensional speckle tracking echocardiography for early detection of myocardial damage in young patients with Fabry disease. *Echocardiography*. 2013;30:1069–1077. doi: 10.1111/echo.12216.

25. Costanzo L, Buccheri S, Capranzano P, Di Pino L, Curatolo G, Rodolico M, Leggio S, Blundo A, Tamburino C, Monte I. Early cardiovascular remodelling in Fabry disease. *J Inherit Metab Dis*. 2014;37:109–116. doi: 10.1007/s10545-013-9607-1.

26. Chareonthaitawee P, Beanlands RS, Chen W, Dorbala S, Miller EJ, Murthy VL, Birnie DH, Chen ES, Cooper LT, Tung RH, White ES, Borges-Neto S, Di Carli MF, Gropler RJ, Ruddy TD, Schindler TH, Blankstein R; NAME OF COLLAB GROUP. Joint SNMMI-ASNC expert consensus document on the role of 18F-FDG PET/CT in cardiac sarcoid detection and therapy monitoring. *J Nucl Med*. 2017;58:1341–1353. doi: 10.2967/jnumed.117.196287.

27. Osborne MT, Hulten EA, Murthy VL, Skali H, Taqueti VR, Dorbala S, DiCarli MF, Blankstein R. Patient preparation for cardiac fluorine-18 fluorodeoxyglucose positron emission tomography imaging of inflammation. *J Nucl Cardiol*. 2017;24:86–99. doi: 10.1007/s12350-016-0502-7.

28. Nacif MS, Arai AE, Lima JA, Bluemke DA. Gadolinium-enhanced cardiovascular magnetic resonance: administered dose in relationship to United States Food and Drug Administration (FDA) guidelines. *J Cardiovasc Magn Reson*. 2012;14:18. doi: 10.1186/1532-429X-14-18.

29. Imbriaco M, Pellegrino T, Piscopo V, Petretta M, Ponsiglione A, Nappi C, Puglia M, Dell'Aversana S, Riccio E, Spinelli L, Pisani A, Cuocolo A. Cardiac sympathetic neuronal damage precedes myocardial fibrosis in patients with Anderson-Fabry disease. *Eur J Nucl Med Mol Imaging*. 2017;44:2266–2273. doi: 10.1007/s00259-017-3778-1.

30. Lang RM, Badano LP, Mor-Avi V, Afilalo J, Armstrong A, Ernande L, Flachskampf FA, Foster E, Goldstein SA, Kuznetsova T, Lancellotti P, Muraru D, Picard MH, Rietzschel ER, Rudski L, Spencer KT, Tsang W, Voigt JU. Recommendations for cardiac chamber quantification by echocardiography in adults: an update from the American Society of Echocardiography and the European Association of Cardiovascular Imaging. *J Am Soc Echocardiogr*. 2015;28:1–39.e14. doi: 10.1016/j.echo.2014.10.003.

31. Spinelli L, Pellegrino T, Pisani A, Giudice CA, Riccio E, Imbriaco M, Salvatore M, Trimarco B, Cuocolo A. Relationship between left ventricular diastolic function and myocardial sympathetic denervation measured by (123)I-meta-iodobenzylguanidine imaging in Anderson-Fabry disease. *Eur J Nucl Med Mol Imaging*. 2016;43:729–739. doi: 10.1007/s00259-015-3273-5.

32. Zizzo C, Monte I, Pisani A, Fatuzzo P, Riccio E, Rodolico MS, Colomba P, Uva M, Cammarata G, Alessandro R, Iemolo F, Duro G. Molecular and clinical studies in five index cases with novel mutations in the GLA gene. *Gene*. 2016;578:100–104. doi: 10.1016/j.gene.2015.12.024.

33. Ishii S, Chang HH, Kawasaki K, Yasuda K, Wu HL, Garman SC, Fan JQ. Mutant alpha-galactosidase a enzymes identified in Fabry disease patients with residual enzyme activity: biochemical characterization and restoration of normal intracellular processing by 1-deoxygalactonojirimycin. *Biochem J*. 2007;406:285–295. doi: 10.1042/BJ20070479.

34. Topaloglu AK, Ashley GA, Tong B, Shabbeer J, Astrin KH, Eng CM, Desnick RJ. Twenty novel mutations in the alpha-galactosidase a gene causing Fabry disease. *Mol Med*. 1999;5:806–811.

35. Shabbeer J, Yasuda M, Luca E, Desnick RJ. Fabry disease: 45 novel mutations in the alpha-galactosidase a gene causing the classical phenotype. *Mol Genet Metab*. 2002;76:23–30.

36. Spada M, Pagliardini S, Yasuda M, Tukel T, Thiagarajan G, Sakuraba H, Ponzone A, Desnick RJ. High incidence of later-onset Fabry disease revealed by newborn screening. *Am J Hum Genet*. 2006;79:31–40. doi: 10.1086/504601.

37. Eng CM, Niehaus DJ, Enriquez AL, Burgert TS, Ludman MD, Desnick RJ. Fabry disease: twenty-three mutations including sense and antisense CpG alterations and identification of a deletional hot-spot in the alpha-galactosidase a gene. *Hum Mol Genet*. 1994;3:1795–1799.

38. Hsu TR, Chang FP, Chu TH, Sung SH, Bizjajeva S, Yu WC, Niu DM. Correlations between endomyocardial biopsies and cardiac manifestations in Taiwanese patients with the Chinese hotspot IVS4+919G>A mutation: data from the Fabry outcome survey. *Int J Mol Sci*. 2017; 18:119.

39. Niemann M, Herrmann S, Hu K, Breunig F, Strotmann J, Beer M, Machann W, Voelker W, Ertl G, Wanner C, Weidemann F. Differences in Fabry cardiomyopathy between female and male patients: consequences for diagnostic assessment. *JACC Cardiovasc Imaging*. 2011;4:592–601. doi: 10.1016/j.jcmg.2011.01.020.

40. Moon JC, Sheppard M, Reed E, Lee P, Elliott PM, Pennell DJ. The histological basis of late gadolinium enhancement cardiovascular magnetic resonance in a patient with Anderson-Fabry disease. *J Cardiovasc Magn Reson*. 2006;8:479–482.

41. Hsu TR, Hung SC, Chang FP, Yu WC, Sung SH, Hsu CL, Dzhagalov I, Yang CF, Chu TH, Lee HJ, Lu YH, Chang SK, Liao HC, Lin HY, Liao TC, Lee PC, Li HY, Yang AH, Ho HC, Chiang CC, Lin CY, Desnick RJ, Niu DM. Later onset Fabry disease, cardiac damage progress in silence: experience with a highly prevalent mutation. *J Am Coll Cardiol*. 2016;68:2554–2563. doi: 10.1016/j.jacc.2016.09.943.

42. Aletras AH, Tilak GS, Natanzon A, Hsu LY, Gonzalez FM, Hoyt RF Jr, Arai AE. Retrospective determination of the area at risk for reperfused acute myocardial infarction with T2-weighted cardiac magnetic resonance imaging: histopathological and displacement encoding with stimulated echoes (DENSE) functional validations. *Circulation*. 2006;113:1865–1870. doi: 10.1161/CIRCULATIONAHA.105.576025.

43. Usman AA, Taimen K, Wasielewski M, McDonald J, Shah S, Giri S, Cotts W, McGee E, Gordon R, Collins JD, Markl M, Carr JC. Cardiac magnetic resonance T2 mapping in the monitoring and follow-up of acute cardiac transplant rejection: a pilot study. *Circ Cardiovasc Imaging*. 2012;5:782–790. doi: 10.1161/CIRCIMAGING.111.971101.

44. Zagrosek A, Abdel-Aty H, Boyé P, Wassmuth R, Messroghli D, Utz W, Rudolph A, Bohl S, Dietz R, Schulz-Menger J. Cardiac magnetic resonance monitors reversible and irreversible myocardial injury in myocarditis. *JACC Cardiovasc Imaging*. 2009;2:131–138. doi: 10.1016/j.jcmg.2008.09.014.

45. Thavendiranathan P, Walls M, Giri S, Verhaert D, Rajagopalan S, Moore S, Simonetti OP, Raman SV. Improved detection of myocardial involvement in acute inflammatory cardiomyopathies using T2 mapping. *Circ Cardiovasc Imaging*. 2012;5:102–110. doi: 10.1161/CIRCIMAGING.111.967836.

46. Friedrich MG, Sechtem U, Schulz-Menger J, Holmvang G, Alakija P, Cooper LT, White JA, Abdel-Aty H, Gutberlet M, Prasad S, Aletras A, Laissy JP, Paterson I, Filipchuk NG, Kumar A, Pauschinger M, Liu P; International Consensus Group on Cardiovascular Magnetic Resonance in Myocarditis. Cardiovascular magnetic resonance in myocarditis: a JACC white paper. *J Am Coll Cardiol*. 2009;53:1475–1487. doi: 10.1016/j.jacc.2009.02.007.

47. Chu GC, Flewitt JA, Mikami Y, Vermes E, Friedrich MG. Assessment of acute myocarditis by cardiovascular MR: diagnostic performance of shortened protocols. *Int J Cardiovasc Imaging*. 2013;29:1077–1083. doi: 10.1007/s10554-013-0189-7.

48. Ozawa K, Funabashi N, Daimon M, Takaoka H, Takano H, Uehara M, Kobayashi Y. Determination of optimum periods between onset of suspected acute myocarditis and 18F-fluorodeoxyglucose positron emission tomography in the diagnosis of inflammatory left ventricular myocardium. *Int J Cardiol*. 2013;169:196–200. doi: 10.1016/j.ijcard.2013.08.098.

49. Nensa F, Kloth J, Tezgah E, Poeppel TD, Heusch P, Goebel J, Nassenstein K, Schlosser T. Feasibility of FDG-PET in myocarditis: comparison to CMR using integrated PET/MRI [published online ahead of print September 8, 2016]. *J Nucl Cardiol*. doi: 10.1007/s12350-016-0616-y.

50. Francone M, Chimenti C, Galea N, Scopelliti F, Verardo R, Galea R, Carbone I, Catalano C, Fedele F, Frustaci A. CMR sensitivity varies with clinical presentation and extent of cell necrosis in biopsy-proven acute myocarditis. *JACC Cardiovasc Imaging*. 2014;7:254–263. doi: 10.1016/j.jcmg.2013.10.011.

51. Nordin S, Kozor R, Bulluck H, Castelletti S, Rosmini S, Abdel-Gadir A, Baig S, Mehta A, Hughes D, Moon JC. Cardiac Fabry disease with late gadolinium enhancement is a chronic inflammatory cardiomyopathy. *J Am Coll Cardiol*. 2016;68:1707–1708. doi: 10.1016/j.jacc.2016.07.741.

52. Shen JS, Meng XL, Moore DF, Quirk JM, Shayman JA, Schiffmann R, Kaneski CR. Globotriaosylceramide induces oxidative stress and up-regulates cell adhesion molecule expression in Fabry disease endothelial cells. *Mol Genet Metab*. 2008;95:163–168. doi: 10.1016/j.ymgme.2008.06.016.

53. Chien Y, Chien CS, Chiang HC, Huang WL, Chou SJ, Chang WC, Chang YL, Leu HB, Chen KH, Wang KL, Lai YH, Liu YY, Lu KH, Li HY, Sung YJ, Jong YJ, Chen YJ, Chen CH, Yu WC. Interleukin-18 deteriorates Fabry cardiomyopathy and contributes to the development of left ventricular hypertrophy in Fabry patients with GLA IVS4+919 G>A mutation. *Oncotarget*. 2016;7:87161–87179. doi: 10.18632/oncotarget.13552.

54. Biancini GB, Jacques CE, Hammerschmidt T, de Souza HM, Donida B, Deon M, Vairo FP, Lourenço CM, Giugliani R, Vargas CR. Biomolecules damage and redox status abnormalities in Fabry patients before and during enzyme replacement therapy. *Clin Chim Acta*. 2016;461:41–46. doi: 10.1016/j.cca.2016.07.016.

55. Hayashi Y, Hanawa H, Jiao S, Hasegawa G, Ohno Y, Yoshida K, Suzuki T, Kashimura T, Obata H, Tanaka K, Watanabe T, Minamino T. Elevated endomyocardial biopsy macrophage-related markers in intractable myocardial diseases. *Inflammation*. 2015;38:2288–2299. doi: 10.1007/s10753-015-0214-1.

56. Rozenfeld P, Feriozzi S. Contribution of inflammatory pathways to Fabry disease pathogenesis. *Mol Genet Metab*. 2017;122:19–27. doi: 10.1016/j.ymgme.2017.09.004.

57. Barbier P, Mirea O, Cefalù C, Maltagliati A, Savioli G, Guglielmo M. Reliability and feasibility of longitudinal AFI global and segmental strain compared with 2D left ventricular volumes and ejection fraction: intra- and inter-operator, test-retest, and inter-cycle reproducibility. *Eur Heart J Cardiovasc Imaging*. 2015;16:642–652. doi: 10.1093/ehjci/jeu274.

58. Farsalinos KE, Daraban AM, Ünlü S, Thomas JD, Badano LP, Voigt JU. Head-to-head comparison of global longitudinal strain measurements among nine different vendors: the EACVI/ASE inter-vendor comparison study. *J Am Soc Echocardiogr*. 2015;28:1171, e2–1181, e2. doi: 10.1016/j.echo.2015.06.011.

59. Bohnen S, Radunski UK, Lund GK, Ojeda F, Looft Y, Senel M, Radziwolek L, Avanesov M, Tahir E, Stehning C, Schnackenburg B, Adam G, Blankenberg S, Muellerleile K. Tissue characterization by T1 and T2 mapping cardiovascular magnetic resonance imaging to monitor myocardial inflammation in healing myocarditis. *Eur Heart J Cardiovasc Imaging*. 2017;18:744–751. doi: 10.1093/ehjci/jex007.

60. Sado DM, White SK, Piechnik SK, Banypersad SM, Treibel T, Captur G, Fontana M, Maestrini V, Flett AS, Robson MD, Lachmann RH, Murphy E, Mehta A, Hughes D, Neubauer S, Elliott PM, Moon JC. Identification and assessment of Anderson-Fabry disease by cardiovascular magnetic resonance noncontrast myocardial T1 mapping. *Circ Cardiovasc Imaging*. 2013;6:392–398. doi: 10.1161/CIRCIMAGING.112.000070.